CT&F - Ciencia, Tecnología y Futuro - Vol. 6 Num. 4 Dec. 2016 Pag. 89 - 106

JOURNAL
CIENCIA, TECNOLOGÍA Y FUTURO

ISSN (Print) 0122-5383
ISSN (Online) 2382-4581

*Journal of oil, gas and alternative energy sources*

# ADSORPTION-DESORPTION OF *n*–$C_7$ ASPHALTENES OVER MICRO- AND NANOPARTICLES OF SILICA AND ITS IMPACT ON WETTABILITY ALTERATION

## *ADSORCIÓN – DESORCIÓN DE n–$C_7$ ASFALTENOS EN MICRO Y NANOPARTÍCULAS DE SÍLICE Y SU IMPACTO EN LA ALTERACIÓN DE LA HUMECTABILIDAD*

## *ADSORÇÃO-DESSORÇÃO DE ASFALTENOS n–$C_7$ SOBRE MICRO E NANOPARTÍCULAS DE SÍLICA E SEU IMPACTO NA ALTERAÇÃO DA MOLHABILIDADE*

Farid B. Cortés[1,2]*; Tatiana Montoya[1]; Sócrates Acevedo[3]; Nashaat N. Nassar[4]* and Camilo Andrés Franco[1,2]*

[1] Grupo de Investigación Fenómenos de Superficie-Michael Polanyi, Facultad de Minas, Universidad Nacional de Colombia Sede Medellín.
[2]Grupo de Investigación en Yacimientos de Hidrocarburos, Facultad de Minas, Universidad Nacional de Colombia Sede Medellín.
[3]Escuela de Química, Facultad de Ciencias, Universidad Central de Venezuela.
[4]Department of Chemical and Petroleum Engineering, University of Calgary, Canada

e-mail: caafrancoar@unal.edu.co
DOI : 10.29047/01225383.06

*(Received: May. 02, 2016; Accepted: Dec 13, 2016)*

**ABSTRACT**

In this work, a study of the adsorption/desorption of *n*–$C_7$ asphaltenes at low and high concentrations (100 – 30000 mg/L) was performed for which the effects of adsorbent particle size (nano and microsilica), pressure, solvent, and temperature were evaluated. Adsorption/desorption tests on different silica surfaces were performed in batch-mode using UV−vis spectrophotometry and thermogravimetric analyses. Owing to its high surface area and dispersibility, nanosilica adsorbed higher quantities of *n*–$C_7$ asphaltenes than microsilica. Asphaltene desorption from nanosilica surface was significant, while the desorption from microsilica surfaces was insignificant, suggesting a higher adsorption potential for the latter. Asphaltene adsorption increased with pressure and decreased with temperature. Type of solvent plays a significant role on the asphaltene desorption. The wettability tests for virgin nanosilica and nanosilica contained adsorbed asphaltenes showed that even at high asphaltene loading, the nanoparticles maintained its water-wet nature.

***Keywords:*** *Adsorption, desorption, asphaltene, reversibility, wettability, silica*

***How to cite:*** Cortés, F. B., Montoya, T., Acevedo, S., Nassar, N. & Franco, A, F. (2016). Adsorption-Desortion of *n*-$C_7$ asphaltenes over micro- and nanoparticles of silica and its impact on wettability alteration. *CT&F - Ciencia, Tecnología y Futuro*, 6(4), 91-106.

**To whom correspondence should be addressed*

## RESUMEN

En este trabajo, se desarrolló un estudio de la adsorción/desorción de asfaltenos a bajas y altas concentraciones (100 – 30000 mg/L) incluyendo el efecto del tamaño de partícula del adsorbente (nano y microsílice), efecto de la presión, de la temperatura y el tipo de solvente. Las pruebas de adsorción/desorción en las diferentes superficies de sílice se realizaron mediante pruebas por lotes usando espectrofotometría UV-vis y análisis termogravimétricos. Debido a sus especiales características de alta área superficial y dispersabilidad, las nanopartículas de sílice adsorben una mayor cantidad de asfaltenos que la sílice microparticulada. Además, se observó que la desorción de los asfaltenos de las nanopartículas de sílice fue significativa, mientras que para el sistema microparticulado fue insignificante, sugiriendo un mayor potencial de adsorción para la sílice microparticulada. La cantidad de asfaltenos adsorbidos aumentó al incrementar la presión, al mismo tiempo que disminuye al aumentar la temperatura del sistema. También, los resultados obtenidos demuestran que el tipo de solvente juega un papel importante en el proceso de desorción de los asfaltenos. Adicionalmente, se realizaron pruebas de humectabilidad para las nanopartículas de sílice en presencia y en ausencia de asfaltenos adsorbidos y se evidenció que incluso a altas cantidades adsorbidas, las nanopartículas mantienen su condición humectable al agua.



***Palabras clave:*** *Adsorción, desorción, asfaltenos, reversibility, humectabilidad, sílice*



## RESUMO

Neste trabalho foi realizado um estudo sobre a adsorção/dessorção de asfaltenos *n*–$C_7$ em concentrações altas e baixas (100 – 30000 mg/L) no intuito de avaliar os efeitos do tamanho da partícula adsorvente (nano e microsílica), pressão, solvente e temperatura. Testes de adsorção/dessorção em diferentes superfícies de sílica foram realizados em série utilizando análises termogravimétricos e de espectrofotometria UV-vis. Vista sua grande área de superfície e capacidade de dispersão, a nanosílica adsorveu maiores quantidades de asfaltenos *n*–$C_7$ do que a microsílica. A dessorção de asfalteno da superfície da microsílica foi insignificante, isso sugere a existência de um maior potencial de adsorção para a microsílica. A adsorção de asfalteno aumentou com a pressão e diminui com a temperatura. O tipo de solvente tem um papel preponderante na dessorção de asfalteno. Os testes de molhabilidade para nanosílica virgem e asfaltenos adsorvidos com conteúdo de nanosílica mostraram que mesmo durante uma carga alta de asfaltenos, as nanopartículas preservaram sua natureza de humidade-agua.



***Palavras-chave:*** *Adsorção, dessorção, asfalteno, reversibilidade, molhabilidade, sílica*

## 1. INTRODUCTION

Wettability is a fundamental reservoir property that affects the flow and spatial distribution of fluids in porous media during oil production and recovery processes, directly influencing the reservoir productivity (du Petrole and Malmaison, 1990; Morrow, 1990). Independent of the origin and mineralogical composition of the porous media, it is believed that most reservoir rocks are initially in a mixed-wet state, neither completely oil-wet nor completely water-wet (Fassi-Fihri, Robin, & Rosenberg, 1995; Salathiel, 1973). However, during different phases of the producing life of a reservoir, wettability can be negatively affected, hence reducing the oil and gas production. The asphaltene potential to alter reservoir wettability has long been recognized (Al-Maamari and Buckley, 2003). Asphaltenes are defined as the most polar heavy compounds of crude oil, and they can be defined by their solubility because they are soluble in light aromatic hydrocarbons, such as toluene, benzene, or pyridine, while they are insoluble in short chain paraffin, such as n-heptane or n-pentane (Groenzin and Mullins, 1999; Mullins, 2010; Mullins, 2011; Mullins, Sheu, Hammami, & Marshall, 2007). A current description establishes that the chemical structure of asphaltenes is generally composed of polyaromatic cores attached to aliphatic chains, and they contain metals, such as vanadium, iron, and nickel, and heteroatoms, such as nitrogen, oxygen, and sulfur (Mullins, 2010). These heteroatoms polar functional groups are primarily responsible for the high dipole moment of asphaltenes promoting asphaltene self-association (Ariza-León, Molina-Velasco, Chaves-Guerrero, 2014; Goual and Firoozabadi, 2002). Asphaltene content in the oil depends on their classification, which is based on the American Petroleum Institute (API) gravity. Thus, in both, heavy and extra heavy oils, an appreciable amount of asphaltenes is found that causes the oil transportation and processing to be complex and challenging. Nevertheless, heavy and extra-heavy crude oils do not present asphaltene precipitation/deposition problems because of resins, which are present in high amounts and act as natural dispersants for asphaltenes (Leontaritis, Amaefule, & Charles, 1994). In contrast, relatively light oils with a low asphaltene content are more prone to asphaltene precipitation/deposition problems, especially in sub-saturated oil reservoirs, which are at pressures above the bubble point (Pedersen, Christensen, & Shaikh, 2014).

Porous media wettability may be altered in reservoirs by asphaltenes via two mechanisms, namely: 1) when the pressure depletion approaches to the asphaltene onset or 2) the adsorption of oil-soluble asphaltene over mineral surfaces. In the first case, several conditions favor the precipitation phenomena, such as gas injection process conditions, as well as changes in the pressure, temperature, and composition of asphaltenes (Al-Maamari and Buckley, 2003). In the second case, oil-soluble asphaltenes are adsorbed onto mineral surfaces, altering the wettability of the oil reservoirs because the asphaltenes are adsorbed onto the rock surface through the polar groups of their molecular structure, leading to the alteration of the rock wettability from water-wetting to oil-wetting, which affects the final oil recovery properties (Dubey and Waxman, 1991).

The understanding of the asphaltene adsorption behavior over solid surfaces is of practical significance for monitoring fluid property variations that commonly occur during oil production due to the wettability alteration. Several experimental studies on asphaltene adsorption on solid surfaces have been reported in the literature (Adams, 2014; González and Moreira, 1991; Marczewski and Szymula, 2002; Marlow, Sresty, Hughes, & Mahajan, 1987; Pernyeszi and Dékány, 2001; Pernyeszi, Patzko, Berkesi, & Dékány, 1998., 1998; Szymula and Marczewski, 2002) to understand the influence of the asphaltene chemical structure and composition (Dudášová, Flåten, Sjöblom, & Øye, 2009; Dudášová, Simon, Hemmingsen, & Sjöblom, 2008), the solvent or precipitant used (Dubey and Waxman, 1991; Nassar, 2010), the surface chemistry (Dudášová *et al*., 2009; Franco, Montoya, Nassar, Pereira-Almao, & Cortés, 2013b. Nassar, 2010; Nassar, Hassan, & Pereira-Almao, 2011a.) and the temperature (Cortés, Mejía, Ruiz, Benjumea, & Riffel, 2012; Franco, Patiño, Benjumea, Ruiz, & Cortés, 2013a; Franco *et al*., 2013b; Nassar, 2010), mainly at low asphaltene concentrations. Moreover, experimental studies regarding asphaltene adsorption have limitations resulting from the complexity of the asphaltene structures (Marczewski and Szymula, 2003; Mendoza de la Cruz *et al*., 2009), which strongly depend on the asphaltene concentration in solution. It is well documented that asphaltenes could be adsorbed onto solid surfaces as molecules, micelles, monomers, dimers and nanoaggregates, depending on the asphaltene concentration in solution, which makes it difficult to understand the asphaltene–asphaltene and

asphaltene aggregate–solid surface (Balabin *et al*., 2011; Franco *et al*., 2013b) interactions at high asphaltene concentrations.

Few asphaltene desorption studies have been reported in the literature (Acevedo, Ranaudo, García, Castillo, & Fernández, 2003; Acevedo *et al*., 2000; Acevedo, Castillo, & Del Carpio, (2014). Adams, 2014; Dubey and Waxman, 1991). Dubey and Waxman (1991) studied the adsorption/desorption of asphaltenes using microparticulate clay minerals, silica, and carbonates as adsorbents and evaluated the effect of adsorbed asphaltenes on the material wettability. The initial asphaltene concentrations evaluated were between 300 and 2500 mg/L. The authors found that for most of the employed desorption solvents, a high degree of irreversible adsorption was observed for kaolin samples (Dubey and Waxman, 1991). They also found that pyridine and the chloroform/methanol azeotrope were the most efficient in the removal of previously adsorbed asphaltenes, with desorption percentages higher than 92%. However, Dubey and Waxman (1991) did not report any desorption study as a function of the system temperature or pressure. Acevedo *et al*. (2014) studied asphaltene desorption in toluene from a silica-based surface. The authors showed an insignificant desorption, suggesting an irreversible adsorption process (Acevedo *et al*., 2003; Acevedo *et al*., 2000). Recently, Acevedo *et al*. (2014) evaluated the capacity of asphaltene desorption from commercial silica plates that had previously adsorbed asphaltenes using toluene as a solvent for both adsorption and desorption steps. The procedure for the adsorption/desorption process consisted of employing commercial silica plates immersed in solutions ranging from 0 to 3000 mg/L of asphaltenes. Then, the sample with adsorbed asphaltenes was removed and immersed again in fresh toluene to measure the desorption. In all cases, the amount desorbed was insignificant. Hence, as proven by the studies above, once asphaltene compounds are adsorbed on the reservoir rock surface, wettability is altered to an oil-wet state until an effective treatment for asphaltene desorption is applied. Recently, nanoparticles have shown high potential for *in-situ* applications in the areas of inhibition of different types of formation damage (Franco, Nassar, Ruiz, Pereira-Almao, & Cortés, 2013c; Hashemi *et al*., 2015; Kazemzadeh, Malayeri, Riazi, & Parsaei, 2015a; Nassar, Betancur, Acevedo, Franco, & Cortés, 2015a; Shayan and Mirzayi, 2015; Zabala *et al*., 2014), enhanced oil recovery (Ehtesabi, Ahadian, & Taghikhani, 2014; Giraldo, Benjumea, Lopera, Cortés, & Ruiz, 2013a; Hashemi, Nassar, & Almao, 2014a; Hashemi, Nassar, & Pereira-Almao, 2012; Hashemi, Nassar, & Pereira Almao, 2013a; Hosseinpour, Mortazavi, Bahramian, Khodatars, & Khodadadi, 2014; Karimi *et al*., 2012; Kazemzadeh *et al*., 2015b) and heavy and extra-heavy oil upgrading (Franco *et al*., 2013b; Franco *et al*., 2014; Franco *et al*., 2015; Hamedi Shokrlu and Babadagli, 2013; Hosseinpour, Khodadadi, Bahramian, & Mortazavi, 2013; Hashemi, Nassar, & Pereira Almao, 2013b; Hashemi, Nassar, & Pereira Almao, 2014b; Mora, Franco, & Cortés, 2013; Nassar *et al*., 2015b; Nassar *et al*., 2012). Regarding the asphaltene-related problems, nanoparticles can restore wettability from an oil-wet state to a water-wet state (Giraldo *et al*., 2013a; Karimi *et al*., 2012). Also, regarding asphaltene precipitation/deposition, nanoparticles can selectively adsorb asphaltenes from large asphaltene aggregate systems, leading to the reduction of the mean asphaltene aggregate size, which subsequently decreases the probability of asphaltene precipitation and deposition (Nassar *et al*., 2015a; Zabala *et al*., 2014). In thermal processes, such as *in-situ* combustion, once asphaltenes are adsorbed on the nanoparticle surface, aquathermolysis or thermolysis, a catalytic cracking of the asphaltene molecule, can occur, leading to the formation of new and lighter compounds that would promote the *in-situ* upgrading of heavy and extra-heavy oils (Franco *et al*., 2013b; Franco *et al*., 2014; Franco *et al*., 2015; Hamedi Shokrlu and Babadagli, 2013; Hashemi *et al*., 2013b; Hashemi *et al*., 2014b; Mora *et al*., 2013; Nassar *et al*., 2015b; Nassar *et al*., 2012; Nassar *et al*., 2011a). However, the re-use of nanoparticles and the changes in their intrinsic properties after asphaltene adsorption are not yet fully understood. Nanoparticles may be recovered under surface conditions from the production fluids (Nassar *et al*., 2012; Nassar *et al*., 2011a; Zabala *et al*., 2014), and depending on the application, they can be regenerated and re-used. Also, regarding the induction of water-wet systems with nanoparticles, asphaltene may be adsorbed over the nanoparticles that are already decorating the porous media and could alter the efficiency of the treatment. Hence, asphaltene desorption to study nanoparticle regeneration is a key parameter that must be understood for a more efficient nanoparticle-based treatment. One green option for nanoparticle regeneration is the catalytic steam gasification of already adsorbed asphaltenes (Franco *et al*., 2014; Hassan *et*

*al*., 2015; Nassar *et al*., 2015b; Nassar *et al*., 2011a). It is expected that under specific temperature conditions, nanoparticles can reduce the temperature of asphaltene decomposition and generate synthetic gas that could be further used as a hydrogen or methane precursor for hydrogenation processes (Franco *et al*., 2014; Hassan *et al*., 2015; Nassar *et al*., 2015b; Nassar *et al*., 2011a).This process would be particularly useful in heavy and extra heavy oil reservoirs. In the case of other reservoirs that experience asphaltene precipitation/deposition problems or that have undergone nanoparticle-based treatments, nanoparticles could be removed with solvents to promote asphaltene desorption.

To the best of our knowledge, reversibility studies of asphaltene adsorption/desorption on the surface of nanoparticles with different asphaltene concentrations have not been reported in the literature. This study is a first attempt to investigate the adsorption/desorption of asphaltene at various initial concentrations (ranging from 0-30000 mg/L). The study also looks into the effects of the following variables on adsorption/desorption process, namely: size of adsorbents, desorption solvents, and commercial asphaltene dispersants, temperature and pressure for simulating asphaltene aggregation and their interaction with the surface. Moreover, the impact of nanoparticles on wettability alteration was addressed. This study provides a better landscape about the suitability of nanosilica candidate for reservoir wettability alteration for enhancing oil recovery application.

## 2. MATERIALS AND METHODS

### *Materials*

Two extra-heavy Colombian crude oils obtained from two different wells of the same reservoir, namely, crude oil A and crude oil B, of 6.2° and 7.2°API with viscosities of 3.5 x $10^6$ and 6.2 x $10^5$ cP at 25°C, respectively, were used as a source of *n*-$C_7$ asphaltenes. The *n*-$C_7$ asphaltene content of crude oil A and crude oil B was 12.6 and 11.5 wt.%, respectively, and was isolated from crude oil by n-heptane (99%, Sigma-Aldrich St. Louis, MO), as explained in previous studies (Franco *et al*., 2013a; Franco *et al*., 2013b).

The *n*-$C_7$ asphaltene samples were named according to the crude oil employed, such as asphaltene A (AspA) and asphaltene B (AspB). The elemental analyses and molecular weight of both *n*-$C_7$ asphaltene samples are showed in Table 1. For the adsorption experiments, toluene (99.5%, MerkK GaG, Germany) was used to re-solubilize extracted *n*-$C_7$ asphaltenes in different mixtures of n-heptane + toluene (Heptol) at 0 (pure toluene), 20 (Heptol 20) and 50 v/v% (Heptol 50). Desorption experiments were conducted using different Heptol mixtures.

**Table 1**. Elemental analysis and molecular weight of n-C7 asphaltenes.

| Parameter | AspA | AspB |
|---|---|---|
| Elemental analysis | | |
| C (wt%) | 81.70 | 81.10 |
| H (wt%) | 7.80 | 7.32 |
| N (wt%) | <0.5% | 1.22 |
| S (wt%) | 6.61 | 2.06 |
| O* (wt%) | 3.56 | 8.30 |
| H/C ratio | 1.14 | 1.08 |
| Molecular weight (g/mol) | 907 | 1826 |

**by difference*

For the desorption experiments, a commercial treatment employed for asphaltene dispersion (CTAD) under reservoir conditions was used. Silica gel nanoparticles (nanosilica) and silica sand microparticles (microsilica) were employed as adsorbents. The nanosilica (Sigma-Aldrich, St. Louis, MO) had a mean particle size of 9 nm with a surface area (SBET) of 389.1 $m^2/g$, as estimated using field emission scanning electron microscopy (FESEM, JSM-6701F, JEOL, Japan) and $N_2$ physisorption at -196°C (Autosorb-1 sortometer, Quantachrome, Boynton Beach, FL) measurements, respectively, as reported in previous works (Nassar *et al*., 2015a). The nanosilica was dried at 120°C before the adsorption experiments to remove any humidity. The microsilica (Minercol S.A., Colombia) size ranged between 425 and 600 μm with a surface area of 3.2 $m^2/g$, as obtained by $N_2$ physisorption at -196°C. Acetone (>99.5%, MerkK GaG, Germany), ethanol (99.9%, Panreac, Spain) and deionized water were used to test the wettability of the nanoparticles.

### *Low-pressure tests*

Batch mode adsorption/desorption experiments were conducted at a pressure of 0.08 MPa and temperatures

of 25 and 80°C for toluene, Heptol 20 and Heptol 50 solutions using nanosilica as the adsorbent. Also, microsilica was used to study the effect of particle size in the *n*-$C_7$ asphaltene adsorption/desorption process.

***Adsorption experiments***

For the adsorption process, a fixed amount of adsorbent (100 mg per 10 mL of model solution) was employed. The *n*-$C_7$ asphaltene model solutions were prepared for different initial concentrations ranging between 100 and 30000 mg/L for all of the mentioned Heptol solutions. For this purpose, *n*-$C_7$ asphaltenes are added to toluene in the desired amount and magnetically stirred for 1 h at 300 rpm. Then, *n*-heptane is added to the solutions to attain the desired concentration of *n*-$C_7$ asphaltenes in the chosen Heptol proportions, and the solution is stirred again for 72 h to ensure *n*-$C_7$ asphaltene stability (Maqbool, Balgoa, & Fogler, 2009; Nassar *et al*., 2015a). Before the adsorption experiments, it was corroborated that the *n*-$C_7$ asphaltenes do not precipitate from the prepared model solutions using the Oliensis spot test number (Asomaning, 2003; Oliensis, 1935) and polarized light microscopy (Franco *et al*., 2015; Mohammadi, Akbarit, Fakhroueian, Bahramian, & Sharareh, A. 2011). Then, model solutions are mixed with the adsorbent and stirred at 200 rpm for 24 h to reach adsorption equilibrium (Franco *et al*., 2013a; Nassar, 2010). The amount adsorbed " $N_{ads}$" (mg/g) is obtained by the difference of the *n*-$C_7$ asphaltene concentration in the bulk phase before ($C_i$) and after ($C_E$) the adsorption process following the mass balance of $N_{ads}=(C_i-C_E)\cdot V/W$, where $V$ ($L$) and $W$ ($g$) are the solution volume and the dry mass of adsorbent, respectively. $C_E$ is measured by using a Genesys 10S UV-vis spectrophotometer (Thermo Scientific, Waltham, MA) (Franco *et al*., 2013b; Franco *et al*., 2015; Nassar, 2010; Nassar *et al*., 2015a). For each Heptol ratio, a calibration curve of absorbance (a.u.) against concentration was constructed at 290 ± 10 nm. Note that after the adsorption process, the adsorbent with adsorbed *n*-$C_7$ asphaltenes was separated from the model solutions by centrifugation for 30 min at 4000 rpm to avoid any noise in the absorbance measurements due to suspended solids (Franco *et al*., 2015). The isotherms obtained by UV-vis spectrophotometry were corroborated through thermogravimetric analyses with a TGA analyzer (Q50, TA Instruments, Inc., New Castle, DE) by heating the adsorbent containing adsorbed asphaltenes in air from 30°C to 700°C at 20°C/min and at a constant airflow rate of 100 $cm^3$/min throughout the experiment. Adsorption experiments were performed in duplicate. Reproducibility of the experiments and uncertainties between the UV-vis and TGA techniques are presented as error bars in the adsorption/desorption isotherms.

***Desorption experiments***

Before the desorption experiments, the adsorbent with adsorbed *n*-$C_7$ asphaltenes is dried at 120°C for 24 h to remove any remaining solvent occurred after the adsorption experiments. Then, this adsorbent is placed in the respective clean Heptol solution and stirred at 200 rpm for 72 h. The effect of the solvent on the value of % *Des* was evaluated using nanosilica with adsorbed *n*-$C_7$ asphaltenes from a Heptol 50 solution at 10000 mg/L and using toluene, Heptol 50 and CTAD as the desorption solvents. The concentration of desorbed *n*-$C_7$ asphaltenes in desorption solvent was determined by colorimetry, and the remaining adsorbed *n*-$C_7$ asphaltenes "$N_{ads,rem}$" (mg/g) was determined as follows (Guzmán *et al*., 2016):

$$N_{ads,rem}=N_{ads}-\frac{C_{E,rem}\cdot V}{W} \qquad (1)$$

where $C_{E,\,rem}$ (mg/L) is the concentration of *n*-$C_7$ asphaltenes in the respective solvent after the desorption process.

Desorption experiments were conducted at 80°C in a tightly sealed glass vials of 0.8 cm diameter and 7 cm length, to prevent solvent evaporation. At this temperature, after the desorption process, the glass vials were placed in dry ice to cool down instantaneously and then carefully opened. After that, the supernatant was quickly decanted to prevent changing the amount desorbed.

***High-pressure tests***

High-pressure tests were performed at 13.8 and 24.1 MPa and 25°C with nanosilica as the adsorbent and for fixed *n*-$C_7$ asphaltene initial concentrations of 1000, 5000 and 10000 mg/L in toluene using a stainless steel displacement cylinder as the vessel (see Figure 1). The cylinder has two independent chambers isolated by a piston. Nanosilica was added to the solutions in the same dosage as that used in the low-temperature tests. In the adsorption process, nanosilica + model solutions were placed in one of the cylindrical chambers, and

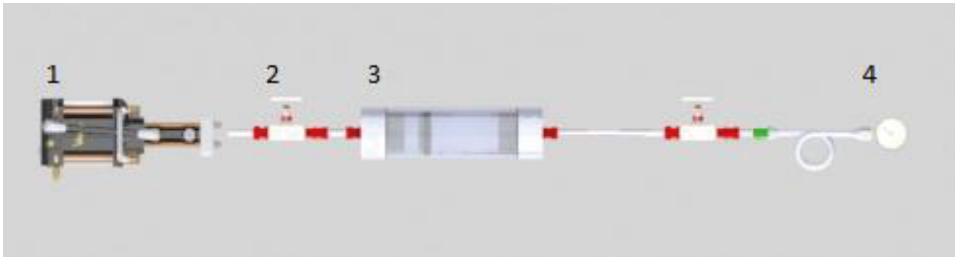


**Figure 1.** Experimental set-up for high-pressure adsorption/desorption tests. 1) The positive displacement pump, 2) a valve, 3) the displacement and 4) the manometer.

the other was filled with mineral oil until the desired pressure was reached; these were left for 24 h. Then, the pressure is alleviated, and nanosilica with adsorbed $n$-$C_7$ asphaltenes are separated. The value of $N_{ads}$ is measured by colorimetry as explained in Section 2.2.1. The recovered solid is then dried at 120°C before the desorption experiments. Desorption was performed by placing the nanosilica with adsorbed $n$-$C_7$ asphaltenes with fresh toluene in the displacement cylinder, and the pressure is increased to 6.9 MPa and maintained for 72 h. Further, toluene with desorbed $n$-$C_7$ asphaltenes is separated from the solid, and $N_{ads,rem}$ is estimated as in Section 2.2.2.

### *Wettability measurements of nanoparticles*

Wettability tests were conducted by contact angle measurements using the sessile drop method (Shang, Flury, Harsh, & Zollars, 2008; Van Oss, 2006). For this purpose, a 2.2-cm long microscope cover glass slide was coated with the selected nanoparticles. First, the glass was cleaned with acetone, deionized water, and ethanol and dried at 120°C for 2 h. Nanoparticles containing different loadings of adsorbed $n$-$C_7$ asphaltenes, after adsorption at different initial concentrations of 10, 100, 1000, 10000 and 30000 mg/L in toluene, were selected. Nanoparticles, with and without adsorbed $n$-$C_7$ asphaltenes, were individually dispersed in ethanol in concentrations of 2% wt/vol and sonicated (Shang *et al*., 2008; Wang, Zhao, & Zhao, 2007). Then, the glass slides are immersed into the nanoparticle suspensions, left to stand for 30 min and carefully withdrawn from the solutions. The coated glasses were further dried at room temperature for 24 h. A droplet of water was placed onto the surface of the dried glass plates using a microsyringe, and then, the contact angle for the different systems at room temperature was estimated using a high definition camera and image analysis software. Contact angle measurements were performed in triplicate for each sample.

## 3. POLANYI'S ADSORPTION POTENTIAL

Polanyi (1914) defined the work required for an adsorbate molecule to be transferred to an adsorbent surface from a given distance as the adsorption potential. The adsorption potential is independent of the temperature for a fixed value of $N_{ads}$, leading to a characteristic curve of an adsorbate – adsorbent system of adsorption potential as a function of $N_{ads}$. The adsorption potential "$A$" for a liquid adsorbate can be defined as follows (Giraldo, Nassar, Benjumea, Pereira-Almao, & Cortés, 2013b; Polanyi, 1914):

$$A = RT \ln\left(1 + \frac{1}{C_E}\right) \qquad (2)$$

with $R$ is the universal ideal gas constant (J/mol·K), and $T$ (K) is the system temperature.

## 4. RESULTS AND DISCUSSION

### *n-$C_7$ asphaltene adsorption/desorption over nano and microsilica*

Panels *a* and *b* in Figure 2 show the adsorption and desorption isotherms of AspA on a) nano and b) microsilica at 25°C in the range of initial concentrations between 100 and 30000 mg/L. The deviation in experimental data was lower than 5%. As seen, nanosilica adsorbed more AspA than the microsilica sample over the entire range of asphaltene concentrations tested, more pronounced at higher concentrations. This behavior is due to the high surface area and dispersibility of nanoparticles relative to the micrometric sample, which presented a $S_{BET}$ value 121 times lower than that of nanosilica. For example, at a $C_E$ of approximately 4700 mg/L, the adsorbed amount of $n$-$C_7$ asphaltenes was approximately 600 mg/g over nanosilica, and for the microsilica sample, the value was 40 mg/g. Adsorption isotherms for the nano and microsilica samples showed an increase in the adsorbed amount of

*n*-$C_7$ asphaltenes as their initial concentration in solution increased. The adsorption isotherms of asphaltenes for nano- and microsilica showed a Type I and II behavior according to the International Union of Pure and Applied Chemistry (IUPAC) classification (Sing, 1985), respectively. In the case of microsilica, for $C_E$ > 10000 mg/L, a multilayer adsorption can be observed. These results are in agreement with previous works reported by our research group (Franco *et al*., 2013b; Franco *et al*., 2014; Franco *et al*., 2015; Franco *et al*., 2013c; Nassar *et al*., 2015c) on the adsorption phenomenon of *n*-$C_7$ asphaltenes onto fumed silica nanoparticles (Franco *et al*., 2013b; Franco *et al*., 2014; Franco *et al*., 2015; Franco *et al*., 2013c) and Ottawa sand (Nassar *et al*., 2015c). At a low concentration of *n*-$C_7$ asphaltenes, the interactions between the coupled *n*-$C_7$ asphaltene – nanoparticles showed a higher affinity than the *n*-$C_7$ asphaltene–microparticles adsorptive pair, as evidenced by the high slope of the adsorption isotherms (Riffel *et al*., 2011). As the asphaltene concentration increases, the Type I isotherms lead to saturation of the available surface area by the *n*-$C_7$ asphaltenes, which results in a plateau for high concentrations through of a multilayer adsorption (Franco *et al*., 2013a; Franco *et al*., 2013b). Type II isotherms have often been described in non-porous materials, which lead to the formation of a multilayer of adsorbate on the microsilica surface (Franco *et al*., 2013a; Franco *et al*., 2013b). As observed, in the range of the low concentrations for the adsorption isotherms, the slope is higher for nanosilica than for microsilica, indicating a higher adsorption affinity for the nanoparticle system (Montoya, Coral, Franco, Nassar, & Cortés, 2014).

For the desorption process, it can be observed from Figure 2 that the desorption isotherm is closer to the vertical axis for the microsilica system than for the nanosilica system, indicating that values of $C_{E,rem}$ are lower for the microparticulate material; hence, the amount of AspA desorbed is lower compared with the nanoparticles. For example, for samples after adsorption from solutions at 300 mg/L using nanosilica, the desorption percentage is 4%, while for the system using microsilica, the value is 0.5%. Even after adsorption with microsilica for initial concentrations of AspA of 30000 mg/L, the desorption percentage is 2.3%. The same trend can be observed for nano- and microsilica for values of $C_E$ < 2000 mg/L. These results explain the severe formation damage caused by asphaltene adsorption because it is hard to remove these compounds from the adsorbed phase (Franco *et al*., 2013c).

Panels a and b in Figure 3 show the comparison of the characteristic curve for the adsorption/desorption process over the nano- and microparticles at 25 ºC and 0.08 MPa. The loops of adsorption and desorption are different, showing a clear case of hysteresis in these isotherms. It is important to mention that the adsorption/desorption phenomena of *n*-$C_7$ asphaltene showed an irreversible process, especially in the case of microsilica in which the desorbed amount is practically null. On

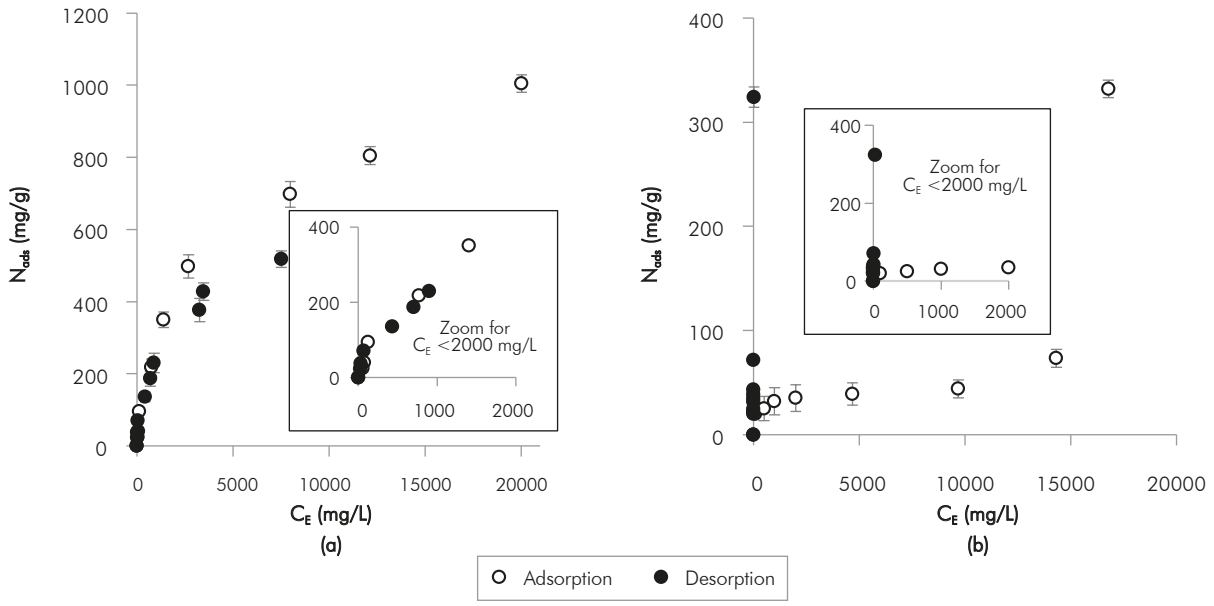


**Figure 2.** Adsorption/desorption isotherms of AspA from toluene on a) nano- and b) microsilica at 25°C and 0.08 MPa.

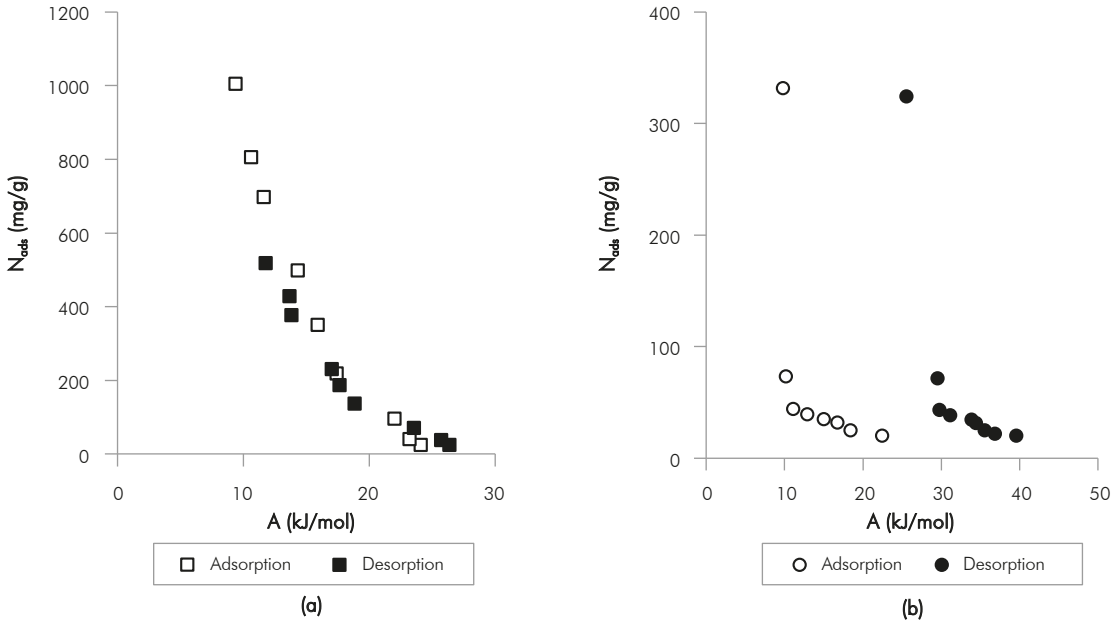


**Figure 3.** Characteristic curves for AspA adsorption/desorption from toluene onto a) nanosilica and b) microsilica at 25°C and 0.08 MPa.

the other hand, for nanosilica, the results reveal a high percentage of desorption of *n*-$C_7$ asphaltenes. Figure 3b shows higher values of A for the desorption process than for the adsorption process for a fixed value of $N_{ads}$. This indicates that the work required for asphaltene molecule to be transferred from the adsorbent surface to the bulk phase is higher than that for the reversed process. However, in Figure 3a, the values of $A$ for desorption are overlapped with the ones for adsorption processes and are even lower for values of $N_{ads} > 300$ mg/g. This supports the high desorption percentage of *n*-$C_7$ asphaltene from nanosilica.

### *Effect of the system pressure*

In this set of experiments, the adsorption/desorption process of AspA over nanoparticles based on a batch mode at a constant temperature of 25°C was evaluated at different pressures of fluid confinement (0.08, 13.8 and 24.1 MPa). Figure 4 shows the adsorption/desorption isotherms of AspA from toluene over nanosilica at a) 13.8 and b) 24.1 MPa. The pressure effect on the adsorption/desorption isotherms showed an increase in the adsorption with pressure over the entire range of concentrations. For example, in the case of adsorption for a fixed value of $C_E$ = 8000 mg/L, the amount

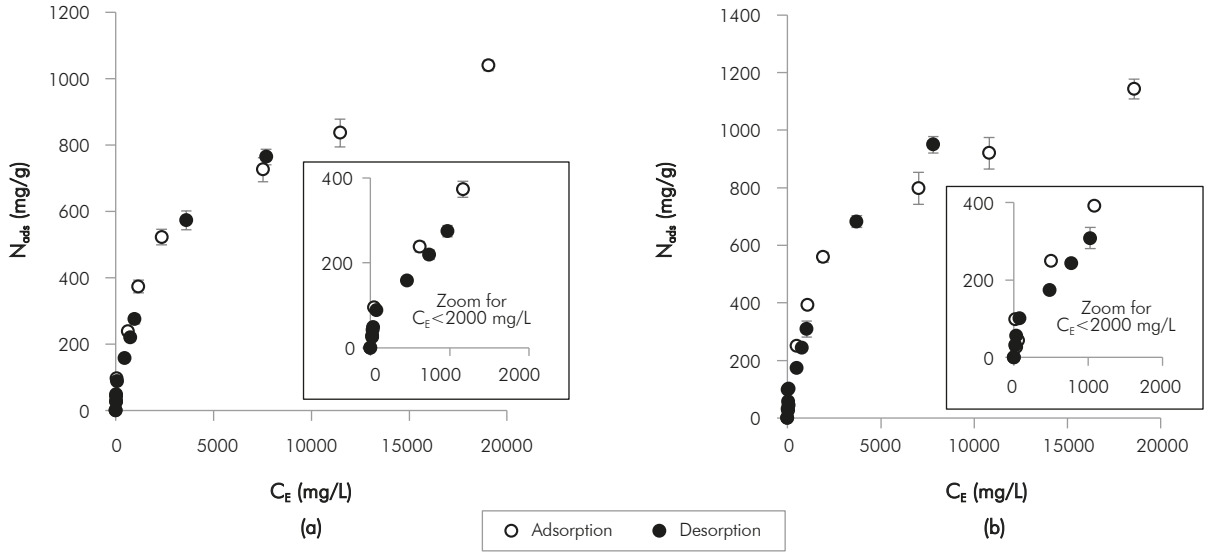


**Figure 4.** Adsorption/desorption isotherms of AspA from toluene onto nanosilica at 25°C and a) 13.8 and b) 24.1 MPa.

adsorbed follows the order 0.08 < 13.8 < 24.1 MPa with values of $N_{ads}$ of 701, 748 and 842 mg/g, respectively. The results are in agreement with those obtained in a previous work for displacement tests (Nassar *et al*., 2015c) in which it was found that asphaltene adsorption over Ottawa sand increased as the system pressure increased. The adsorption and desorption isotherms at high pressures clearly showed a behavior similar to that obtained at 0.08 MPa, showing a Type I isotherm based on IUPAC (Sing, 1985). This behavior is more pronounced at a high concentration of *n*-$C_7$ asphaltenes, mainly for the desorption loop. Meanwhile, at low concentrations, the difference is almost null and could be explained by the increase in asphaltene solubility as the pressure is increased (Bai and Bai, 2005). This is not surprising because the asphaltene solubility is a function of pressure (Bai and Bai, 2005) and is expected to increase as the pressure increases and as the fluid density increases. High pressures have significant implications on the chemical potential of a liquid phase, where it deviates from ideality. At low pressures, the association of self-associative molecules can be neglected. However, as the system pressure increases, the forces between the molecules could be considered to be chemical instead of physical in nature leading to the strengthening of intermolecular interactions such as hydrogen bonds, dispersion forces, induction forces, and electrostatic forces between adsorbate-adsorbate, which may also lead to an increase in the affinity between AspA and the solid surface (Nassar *et al*., 2015c).

### *Effect of the solvent on desorption*

Panels a to d in Figure 5 show the adsorption/desorption isotherms and characteristic curves for AspA using nanosilica as the adsorbent and for a, b) Heptol 20 and c, d) Heptol 50 solutions, respectively, under temperature and pressure conditions of 25°C and 0.08 MPa, respectively. As seen in Figure 5, the amount of AspA adsorbed from different solvents increased in the following order: toluene < Heptol 20 < Heptol 50. However, at low concentrations, the differences among the solvents are not significant, while at high concentrations, they are substantial. This behavior can be explained by the aggregation phenomena of asphaltenes, which depends on the adsorbate concentration, temperature, and pressure. Note that asphaltene aggregates that are in contact with adsorbent are adsorbed immediately in the highly energetic particle sites. At high concentrations, multilayer adsorption can be explained because of the asphaltene–asphaltene interaction becomes more important than the asphaltene–surface interactions. These results are in agreement with those reported by Franco *et al*. (2015) and Nassar *et al*. (2015a) who showed the effect of the *n*-$C_7$ asphaltene aggregation using different solvents and particles. It is expected that as the amount of *n*-heptane increases, the capacity of the solvent to solubilize the *n*-$C_7$ asphaltenes is reduced, thus promoting polar, dispersion and hydrogen bonding interactions between the different functional groups in their structure (Spiecker, Gawrys, & Kilpatrick, 2003a; Spiecker, Gawrys, Trail, & Kilpatrick, 2003b). Also, the ratio of polar/non-polar moieties in the *n*-$C_7$ asphaltene structure defines the polarity (Pernyeszi *et al*., 1998; Spiecker *et al*., 2003a) and leads to either a less or more favorable self-association phenomena (Montoya *et al*., 2014).

The desorption process was performed after the occurrence of the adsorption phenomena. For the Heptol 20 and Heptol 50 systems, a percentage of AspA asphaltene desorption was observed. This desorption behavior of *n*-$C_7$ asphaltenes can be explained by the data presented in Figures 5b and 5d in which it can be observed that the values of $A$ for the adsorption and desorption processes are similar for a fixed value of $N_{ads}$. The AspA desorption decreased as the amount of *n*-heptane decreased. For example, for initial AspA concentrations of 1000, 10000 and 30000 mg/L, the desorption percentage in the Heptol 20 system was 13, 18 and 21%, while for the Heptol 50 system, the desorption percentage for the same initial concentrations was 8, 12 and 17%, respectively. This could be because the asphaltene solubility power is reduced as the amount of *n*-heptane in the system increases (Nassar *et al*., 2015c) in addition to the increased fraction of highly polar moieties that could have a higher affinity towards the nanoparticles surface. These results are evident from the slope of the desorption isotherms at low concentrations, which tend to increase as the amount of *n*-heptane in the solution increases, indicating that *n*-$C_7$ asphaltenes prefer to stay in the adsorbed phase rather than in the bulk phase (Montoya *et al*., 2014).

An additional desorption test was conducted by varying the desorbing solvent after AspA adsorption onto nanosilica from Heptol 50 solutions at an initial *n*-$C_7$ asphaltene concentration of 10000 mg/L and by fixing the test temperature and pressure to 25°C and 0.08 MPa, respectively. Figure 6 shows the desorption

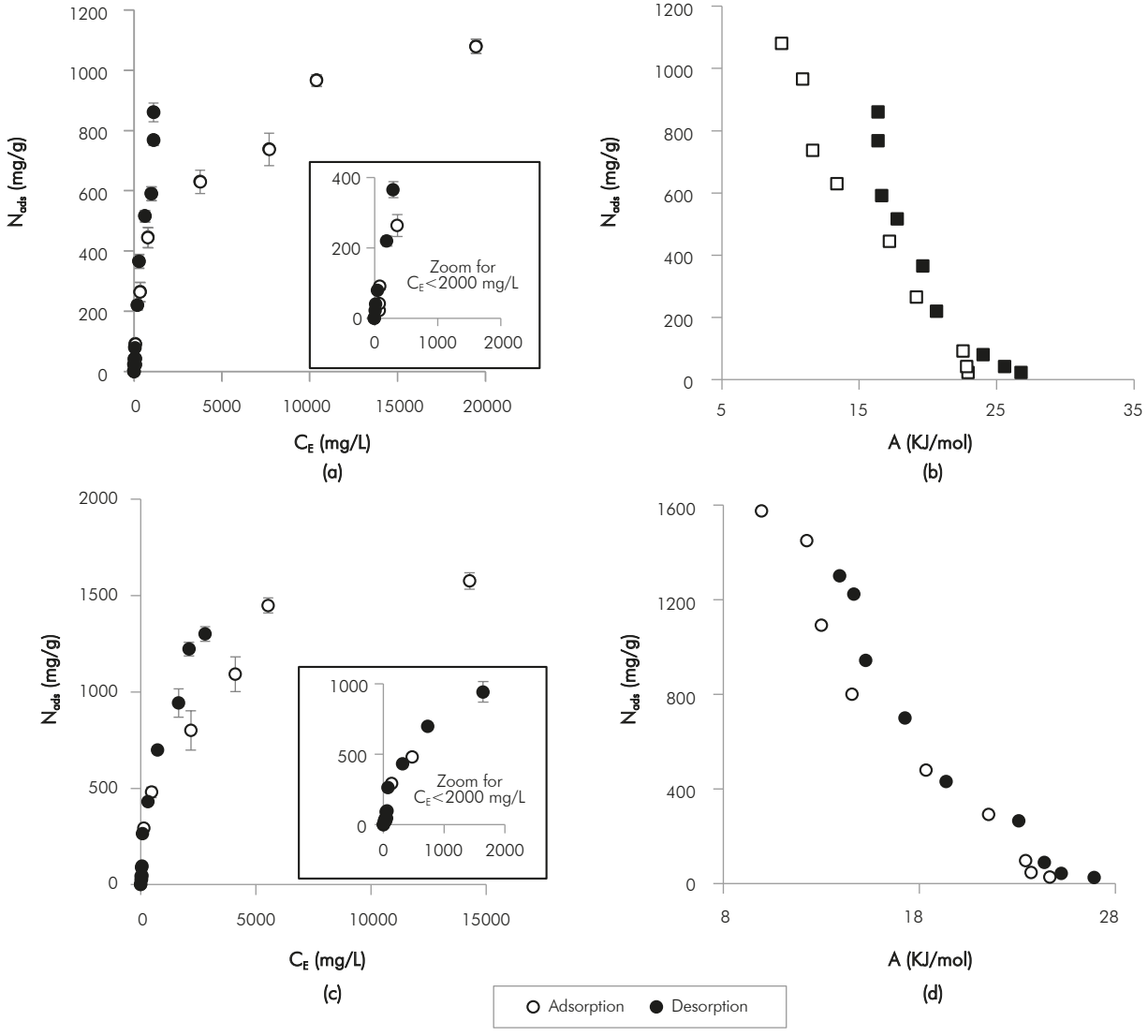


**Figure 5**. Adsorption/desorption isotherms and characteristic curves of AspA from a, b) Heptol 20 and c, d) Heptol 50 solutions, respectively, using nanosilica as the adsorbent under temperature and pressure conditions of 25°C and 0.08 MPa.

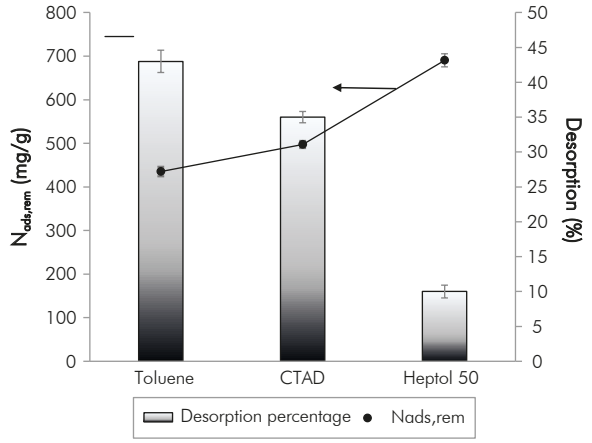


**Figure 6**. AspA desorption from nanosilica using toluene, CTAD and Heptol 50 as desorbing solvents for an initial concentration of 10000 mg/L, temperature 25°C and pressure 0.08 MPa.

percentages of AspA from nanosilica using different desorbing types of solvents. As seen in Figure 6, the values of $N_{ads,rem}$ increase in the order of toluene < CTAD < Heptol 50 with desorption percentages of 43, 35 and 10%, respectively. Higher desorption percentages for toluene compared with Heptol 50 indicate that the desorption process of AspA from the nanosilica surface is strongly dependent on the solubility power of the desorption solvent employed. The *n*-$C_7$ asphaltene desorption using the CTAD treatment was lower than that for toluene and could be because this product is a mixture of different solvents; hence, the solubility power could be reduced compared with a pure aromatic compound.

### *Effect of the temperature on n-$C_7$ asphaltene desorption*

AspA desorption was conducted at 80°C in closed systems for samples after the adsorption processes at 25°C and 0.08 MPa using nanosilica as the adsorbent. Figure 7 shows the obtained desorption isotherms of AspA from nanosilica. As seen, the values of $N_{ads,rem}$ follow the order of Heptol 50 > Heptol 20 > toluene, indicating that even at different temperatures, the trend as a function of the amount of precipitant is maintained. Also, when comparing the desorption at 80°C with the results at 25°C (Figure 5), it can be seen that an extra amount of AspA is extracted from the adsorbed phase, indicating that increasing the temperature promotes the *n*-$C_7$ asphaltene desorption. Changes in temperature may influence the asphaltene aggregate size in the solution, altering their spatial disposition over the adsorbent surface and decreasing the intermolecular forces between the adsorbent and the adsorbate (Franco *et al*., 2014; Nassar, 2010; Nassar *et al*., 2015c). Also, as the temperature is increased, the liquid density decreased (Wu, Prausnitz, & Firoozabadi, 1998), and the power of the solvent to dissolve the asphaltenes decreased, directly affecting their molar volume, which tends to increase with temperature (Diallo, Cagin, Faulon, & Goddard, 2000).

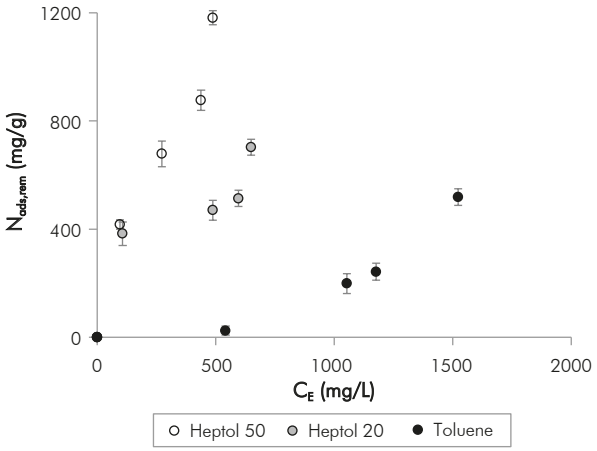


**Figure 7.** AspA desorption isotherms from nanosilica at temperature 80°C and pressure 0.08 MPa.

### *Effect of the temperature on n-$C_7$ asphaltene desorption*

As the chemical nature of asphaltene may differ depending on the crude oil source, AspB was employed to evaluate the effect of the *n*-$C_7$ asphaltene origin on the desorption process. Experiments were conducted for a fixed initial AspB concentration of 10000 mg/L in toluene, Heptol 20 and Heptol 50 at 25°C and 0.08 MPa.

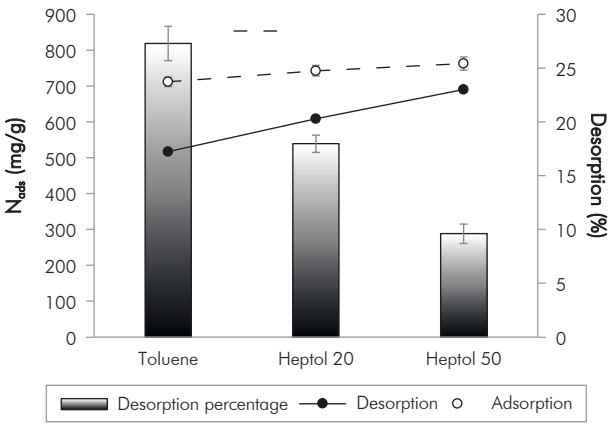


**Figure 8.** AspB adsorption/desorption over nanosilica using toluene, Heptol 20 and Heptol 50 for a fixed initial concentration of 10000 mg/L and temperature and pressure conditions of 25°C and 0.08 MPa, respectively.

Figure 8 shows the results of the adsorption/desorption process of AspB over nanosilica. As expected, the amount adsorbed increased in the order of toluene < Heptol 20 < Heptol 50. A similar trend can be observed for $N_{ads,rem}$. The desorption percentage for the Heptol 20 and Heptol 50 solutions was 18 and 10%, which was closer to the ones obtained for AspA. However, the desorption percentage of AspB using toluene was 27%, which was approximately 16% lower than that of AspA and could be due to the different degrees of self-association for each asphaltene. As it can be seen from Table 1, AspB differs from AspA mainly in the heteroatoms content and the molecular weight. Lower desorption percentages for AspB may be associated with the higher polarity and higher adsorbate-adsorbate interaction on the adsorbent surface ruled mainly by π−π stacking, and acid−base interactions between the O-, and/or N-containing functional groups.

### *Nanoparticle wettability before and after n-$C_7$ asphaltene adsorption*

The wettability test of the nanoparticles was conducted to better understand the wetting state of the nanoparticles after the adsorption of *n*-$C_7$ asphaltenes. Thus, it is of primary importance to know the effect of adsorbed asphaltenes on altering the wetting properties of the nanoparticles, especially for practical application, like treatments designed to restore/alter reservoir wettability. Figure 9 shows photographs of a water droplet over the nanosilica-coated glass for the nanosilica a) before and after AspA adsorption from toluene at initial concentrations of b) 1000, c) 10000 and d) 30000 mg/L. The estimated mean contact angles

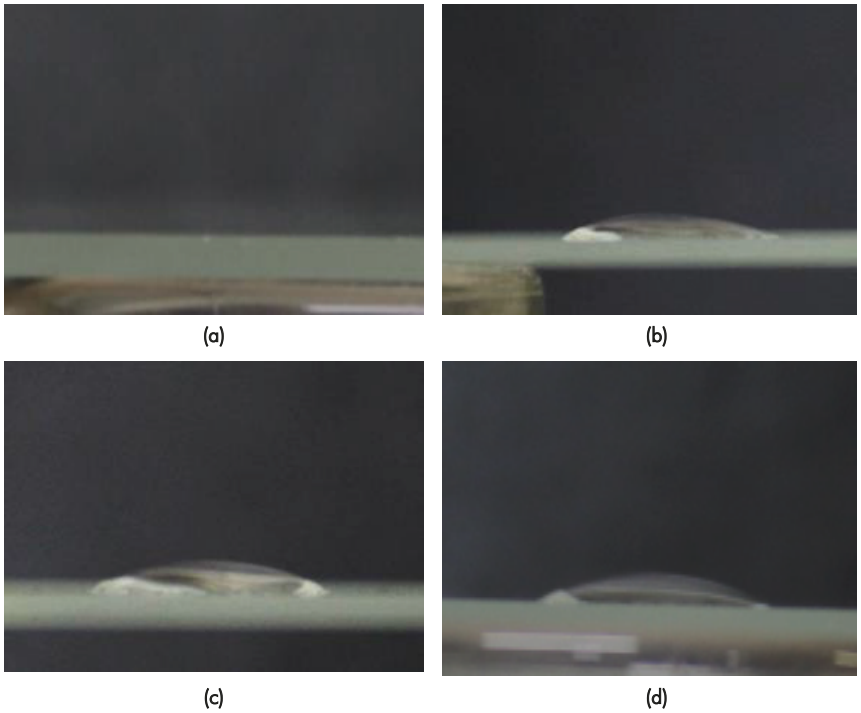


**Figure 9**. . Photographs of water droplets over the nanosilica-coated glass for the nanosilica a) before and after AspA adsorption from toluene at initial concentrations of b) 1000, c) 10000 and d) 30000 mg/L.

for the nanosilica before and after AspA adsorption at different initial concentrations are shown in Figure 10. As seen, in Figures 9 and 10, no water droplet is obtained for the nanoparticles without AspA adsorption, indicating a strongly water-wetted surface. A similar situation can be observed for nanosilica after AspA adsorption at $C_i$ = 100 mg/L. At this initial concentration, it is believed that asphaltene molecules do not occupy all the nanosilica available active sites for adsorption. Hence, still water would be more prone to interact with the nanoparticle surface. For the cases of higher initial concentrations of 1000, 10000 and 30000 mg/L, a water droplet forms with mean contact angles of 21.3, 31.1 and 30.5°, respectively. This suggests that even for large amounts of AspA, the wettability state of the nanosilica remains water-wetted but not as strong as for virgin nanosilica. The droplet formation could be because AspA is adsorbed onto the surface through the polar functional groups, and hence the non-polar functional groups are exposed outwards. However, at high AspA concentrations (i.e., 10000 and 30000 mg/L) the surface is not completely oil-wetted because AspA may form multilayers over the nanosilica surface and the outer layer would be formed by AspA adsorption through the firstly formed non-polar, and hence the polar parts could be exposed outwards as well and would interact with the water. Worth noting here that, within the range of asphaltene concentrations evaluated, the surface wettability of silica nanoparticles do not change significantly, even at high asphaltene concentrations, suggesting that these types of nanoparticles are suitable for wettability alteration treatments in enhanced oil recovery application.

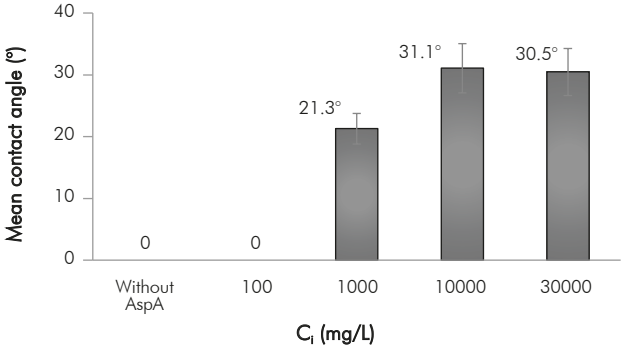


**Figure 10**. Estimated mean contact angles for the nanosilica before and after AspA adsorption from toluene at initial concentrations of 100, 1000, 10000 and 30000 mg/L.

## 5. CONCLUSIONS

- In this study, adsorption and desorption isotherms of *n*-$C_7$ asphaltenes over micro- and nanosilica were successfully evaluated. Nanosilica showed higher *n*-$C_7$ asphaltene adsorption than microsilica because

of its high extent of dispersibility and exposed surface area available for adsorption. Asphaltene desorption was also higher for nanosilica than microparticles. The loops of adsorption and desorption are different, showing a clear case of hysteresis in the obtained isotherms; this could be because the work required for an adsorbate molecule to be transferred from the adsorbent surface to the bulk phase is higher than for the opposite process, as estimated by Polanyi's adsorption potential. Asphaltene desorption decreased by increasing the amount of precipitant in heptol solutions, due to the decreased solubility of asphaltenes. The results at high pressures of 13.8 and 24.1 MPa showed that asphaltene adsorption is slightly increased by increasing the system pressure. The amount desorbed increased in the order of 0.08 > 13.8 > 24.1 MPa. Also, desorption processes at 80°C demonstrated that the amount desorbed increased with temperature regardless of the types of solvent employed.

- Nanosilica surface wettability was not significantly impacted by asphaltene adsorption, and it maintained its water-wet nature, regardless of the asphaltene loadings. This suggests that nanoparticles are suitable for reservoir wettability alteration treatment for enhancing oil recovery.

## ACKNOWLEDGEMENTS

The authors want to acknowledge to the Departamento Administrativo de Ciencia, Tecnología e Innovación (COLCIENCIAS), ECOPETROL S.A and Universidad Nacional de Colombia for the support provided in Agreement 264 of 2013 and the Cooperation Agreement 04 of 2013, respectively. Thanks are due to Miss Maria Alejandra Giraldo and Mónica Lozano for their fruitful support. The authors are also grateful to the Natural Sciences and Engineering Research Council of Canada (NSERC) for the financial support provided through the NSERC discovery grant for Dr. Nassar.

## REFERENCES

Acevedo, S., Ranaudo, M. A., García, C., Castillo, J., & Fernández, A. (2003). Adsorption of asphaltenes at the toluene-silica interface: a kinetic study. *Energ. Fuel*., 17 (2), 257-261. DOI: 10.1021/ef020104q.

Acevedo, S., Ranaudo, M. A., García, C., Castillo, J., Fernández, A., Caetano, M., & Goncalvez, S. (2000). Importance of asphaltene aggregation in solution in determining the adsorption of this sample on mineral surfaces. *Colloid. Surf.* A., 166 (1-3), 145-152. DOI: http://dx.doi.org/10.1016/S0927-7757(99)00502-6.

Acevedo, S. C., Castillo, J., & Del Carpio, E. H. N., (2014). Precipitation of asphaltenes and resins at the Toluene– Silica interface: an example of precipitation promoted by local electrical fields present at the Silica–Toluene interface. *Energ. Fuel*., 28 (8), 4905-4910. DOI: 10.1021/ef5008984.

Adams, J. J., (2014). Asphaltene Adsorption, a literature review. *Energ. Fuel*., 28 (5), 2831-2856. DOI: 10.1021/ef500282p.

Al-Maamari, R. S. & Buckley, J. S. (2003). Asphaltene precipitation and alteration of wetting: the potential for wettability changes during oil production. SPE Reserv. *Eval. Eng*., 6 (4): 210-214. DOI: https://doi.org/10.2118/84938-PA

Ariza-León, E., Molina-Velasco, D. R., Chaves-Guerrero, A. (2014) Review of studies on asphaltene-wax interaction and the effect threreof on crystallization. *CT&F -Cienc. Tecnol. Fut*., 5 (5), 39-53.

Asomaning, S., (2003). Test methods for determining asphaltene stability in crude oils. *Pet. Sci. Technol.* , 21 (3-4), 581-590. DOI: http://dx.doi.org/10.1081/LFT-120018540.

Bai, Y. & Bai, Q. (2005). *Subsea pipelines and risers.* Elsevier.

Balabin, R. M., Syunyaev, R. Z., Schmid, T., Stadler, J., Lomakina, E. I., & Zenobi, R. (2010). Asphaltene adsorption onto an iron surface: combined near-infrared (NIR), Raman, and AFM study of the kinetics, thermodynamics, and layer structure. *Energ. Fuel*., 25 (1), 189-196. DOI: 10.1021/ef100779a.

Cortés, F. B., Mejía, J. M., Ruiz, M. A., Benjumea, P. & Riffel, D. B. (2012). Sorption of asphaltenes onto nanoparticles of nickel oxide supported on nanoparticulated silica gel. *Energ. Fuel*., 26 (3): 1725-1730. DOI: 10.1021/ef201658c

Diallo, M., Cagin, T., Faulon, J., & Goddard, W. (2000). *Chapter 5 in Asphaltenes and Asphalts*, 2. Developments in Petroleum Science B, 40: 103-125.

Du Petrole, F., & Malmaison, F. R., (1990). *Evaluation of reservoir wettability and its effect on oil recovery, Interfacial Phenomena in Petroleum Recovery.* Boca Raton: CRC Press.

Dubey, S., & Waxman, M., (1991). Asphaltene adsorption and desorption from mineral surfaces. *SPE Reservoir Eng*., 6 (03), 389-395. DOI: 10.2118/18462-PA.

Dudášová, D., Flåten, G. R., Sjöblom, J., & Øye, G. (2009). Study of asphaltenes adsorption onto different minerals and clays: Part 2. Particle characterization and suspension stability. *Colloid. Surf.* A, 335 (1-3), 62-72. DOI: http://dx.doi.org/10.1016/j.colsurfa.2008.10.041.

Dudášová, D., Simon, S., Hemmingsen, P. V. & Sjöblom, J., (2008). Study of asphaltenes adsorption onto different minerals and clays: Part 1. Experimental adsorption with UV depletion detection. *Colloid. Surf.* A, 317(1-3): 1-9. DOI: http://dx.doi.org/10.1016/j.colsurfa.2007.09.023.

Ehtesabi, H., Ahadian, M. M. & Taghikhani, V. (2014). Enhanced heavy oil recovery using TiO2 nanoparticles: investigation of deposition during transport in core plug. *Energ. Fuel*., 29 (1), 1-8. DOI: 10.1021/ef5015605.

Fassi-Fihri, O., Robin, M., & Rosenberg, E. (1995). Wettability studies at the pore level: a new approach by the use of cryo-scanning electron microscopy. *SPE Format. Eval*., 10 (01), 11-19. DOI: https://doi.org/10.2118/22596-PA.

Franco, C., Patiño, E., Benjumea, P., Ruiz, M.A., & Cortés, F. B., (2013a). Kinetic and thermodynamic equilibrium of asphaltenes sorption onto nanoparticles of nickel oxide supported on nanoparticulated alumina. *Fuel*, 105, 408-414. DOI: http://dx.doi.org/10.1016/j.fuel.2012.06.022.

Franco, C. A., Montoya, T., Nassar, N. N., Pereira-Almao, P., & Cortés, F. B., (2013b). Adsorption and subsequent oxidation of Colombian asphaltenes onto nickel and/or palladium oxide supported on fumed silica nanoparticles. *Energ. Fuel*., 27 (12), 7336-7347. DOI: 10.1021/ef4018543.

Franco, C. A., Nassar, N. N., Montoya, T., & Cortés, F. B., (2014). *NiO and PdO Supported on fumed silica nanoparticles for adsorption and catalytic steam gasification of Colombian C7 asphaltenes*. In: J. Ambrosio, Handbook on Oil Production Research. Nova Science Publishers.

Franco, C. A., Nassar, N. N., Montoya, T., Ruíz, M. A., & Cortés, F. B. (2015). Influence of asphaltene aggregation on the adsorption and catalytic behavior of nanoparticles. *Energ. Fuel*., 29 (3), 1610-1621. DOI: 10.1021/ef502786e.

Franco, C. A., Nassar, N. N., Ruiz, M. A., Pereira-Almao, P., & Cortés, F. B., (2013c). Nanoparticles for inhibition of asphaltenes damage: adsorption study and displacement test on porous media. *Energ. Fuel*., 27 (6), 2899-2907. DOI: 10.1021/ef4000825.

Giraldo, J., Benjumea, P., Lopera, S., Cortés, F. B., & Ruiz, M. A., (2013a). Wettability alteration of sandstone cores by alumina-based nanofluids. *Energ. Fuel*., 27 (7): 3659-3665. DOI: 10.1021/ef4002956.

Giraldo, J., Nassar, N. N., Benjumea, P., Pereira-Almao, P., & Cortés, F.B., (2013b). Modeling and prediction of asphaltene adsorption isotherms using Polanyi's modified theory. *Energ. Fuel*., 27 (6), 2908-2914. DOI: 10.1021/ef4000837.

González, G., & Moreira, M. B., (1991). The wettability of mineral surfaces containing adsorbed asphaltene. *Colloid. Surf*., 58 (3), 293-302. DOI: https://doi.org/10.1016/0166-6622(91)80229-H.

Goual, L., & Firoozabadi, A., (2002). Measuring asphaltenes and resins, and dipole moment in petroleum fluids. *AIChE J*., 48 (11), 2646-2663. DOI: 10.1002/aic.690481124.

Groenzin, H., & Mullins, O. C., (1999). Asphaltene molecular size and structure. *J. Phys. Chem. A*, 103 (50), 11237-11245 DOI: 10.1021/jp992609w.

Guzmán, J. D., Betancur, S., Carrasco-Marín, F., Franco, C. A., Nassar, N. N. & Cortés, F. B. (2016). Importance of the adsorption method used for obtaining the nanoparticle dosage for asphaltene-related treatments. *Energ. Fuel*., 20 (3), 2052-2059. DOI: 10.1021/acs.energyfuels.5b02841.

Hamedi Shokrlu, Y. & Babadagli, T., (2013). In-situ upgrading of heavy oil/bitumen during steam injection by use of metal nanoparticles: a study on in-situ catalysis and catalyst transportation. SPE Reserv. *Eval. Eng*., 16 (3), 333-344.

Hashemi, R., Nassar, N. N. & Almao, P. P., (2014a). Nanoparticle technology for heavy oil *in-situ* upgrading and recovery enhancement: opportunities and challenges. *App. Energ.,* 133, 374-387.

Hashemi, R., Nassar, N. N., & Pereira-Almao, P. (2012). Transport behavior of multimetallic ultradispersed nanoparticles in an oil-sands-packed bed column at a high temperature and pressure. *Energ. Fuel*., 26 (3): 1645-1655. DOI: 10.1021/ef201939f.

Hashemi, R., Nassar, N. N., & Pereira Almao, P., (2013a). Enhanced heavy oil recovery by in situ prepared ultradispersed multimetallic nanoparticles: a study of hot fluid flooding for Athabasca bitumen recovery. *Energ. Fuel*., 27 (4): 2194-2201. DOI: 10.1021/ef3020537.

Hashemi, R., Nassar, N. N. & Pereira Almao, P., (2013b). In situ upgrading of athabasca bitumen using multimetallic ultradispersed nanocatalysts in an oil sands packed-bed column: Part 1. Produced liquid quality enhancement. *Energ. Fuel*., 28 (2), 1338-1350. DOI: 10.1021/ef401716h.

Hashemi, R., Nassar, N. N. & Pereira Almao, P., (2014b). In situ upgrading of athabasca bitumen using multimetallic ultradispersed nanocatalysts in an oil sands packed-bed column: Part 2. Solid analysis and gaseous product distribution. *Energ. Fuel*., 28 (2): 1351-1361. DOI: 10.1021/ef401719n.

Hashemi, S. I., Fazelabdolabadi, B., Moradi, S., Rashidi, A. M., Shahrabadi, A., & Bagherzadeh, H. (2015). On the application of NiO nanoparticles to mitigate in situ asphaltene deposition in carbonate porous matrix . *Appl. Nanosci*., 6 (1), 71-81. DOI: 10.1007/s13204-015-0410-1.

Hassan, A., Carbognani-Arambarri, L., Nassar, N. N., Vitale, G., Lopez-Linares, F., & Pereira-Almao, P. (2015). Catalytic steam gasification of n-C 5 asphaltenes by kaolin-based catalysts in a fixed-bed reactor. *App. Catal. A-Gen*., 507, 149-161. DOI: 10.1016/j.apcata.2015.09.025.

Hosseinpour, N., Khodadadi, A. A., Bahramian, A., & Mortazavi, Y. (2013). Asphaltene adsorption onto acidic/basic metal oxide nanoparticles toward in situ upgrading of reservoir oils by nanotechnology. *Langmuir,* 29 (46), 14135-14146. DOI: 10.1021/la402979h.

Hosseinpour, N., Mortazavi, Y., Bahramian, A., Khodatars, L., & Khodadadi, A. A., (2014). Enhanced pyrolysis and oxidation of asphaltenes adsorbed onto transition metal oxides nanoparticles towards advanced *in-situ* combustion EOR processes by nanotechnology. *App. Catal. A-Gen*., 477: 159-171. DOI: http://dx.doi.org/10.1016/j.apcata.2014.03.017.

Ju, B., Fan, T., & Ma, M. (2006). Enhanced oil recovery by flooding with hydrophilic nanoparticles. *China Part*., 4 (1): 41-46. DOI: https://doi.org/10.1016/S1672-2515(07)60232-2.

Karimi, A., Fakhroueian, Z., Bahramian, A., Khiabanit, N. O., Darabad, J. B., Azin, R., & Aria, S. (2012). Wettability alteration in carbonates using zirconium oxide nanofluids: EOR implications. *Energ. Fuel*., 26 (2), 1028-1036. DOI: 10.1021/ef201475u.

Kazemzadeh, Y., Eshraghi, E., Kasemi, K., Sourani, S, Mehrabi, M., & Ahmadi, Y. (2015b). Behavior of asphaltene adsorption onto the metal oxide nanoparticle surface and Its effect on heavy oil recovery. *Ind. Eng. Chem. Res*., 54 (1), 233-239. DOI: 10.1021/ie503797g.

Kazemzadeh, Y., Malayeri, M. R., Riazi, M., & Parsaei, R. (2015a). Impact of Fe3O4 nanoparticles on asphaltene precipitation during CO 2 injection. *J. Nat. Gas Sci. Eng*., 22, 227-234. DOI: http://dx.doi.org/10.1016/j.jngse.2014.11.033.

Leontaritis, K., Amaefule, J., & Charles, R.(1994). A systematic approach for the prevention and treatment of formation damage caused by asphaltene deposition. *SPE Prod. Facil*., 9 (3), 157-164.

Maqbool, T., Balgoa, A. T., & Fogler, H. S. (2009). Revisiting asphaltene precipitation from crude oils: a case of neglected kinetic effects. *Energ. Fuel*,. 23 (7): 3681-3686. DOI: 10.1021/ef9002236.

Marczewski, A., & Szymula, M. (2003). Adsorption of asphaltenes from toluene on quartz and silica-rich soils. *Adsorption,* 58(4), 70-79.

Marczewski, A. W., & Szymula, M. (2002). Adsorption of asphaltenes from toluene on mineral surface. *Colloid. Surf.* A, 208 (1-3), 259-266. DOI: http://dx.doi.org/10.1016/S0927-7757(02)00152-8.

Marlow, B., Sresty, G., Hughes, R., & Mahajan, O. (1987). Colloidal stabilization of clays by asphaltenes in hydrocarbon media. *Colloid. Surf.*, 24 (4), 283-297. DOI: https://doi.org/10.1016/0166-6622(87)80235-4.

Mendoza de la Cruz, J. L., Castellanos-Ramírez, I. V., Ortiz-Tapiac, A. O., Buenrostro-González, E., Durán-Valencia,

C., & López-Ramírez, S. (2009). Study of monolayer to multilayer adsorption of asphaltenes on reservoir rock minerals. *Coll. Surf. A*., 340(1), 149-154. DOI: 10.1016/j.colsurfa.2009.03.021

Mohammadi, M., Akbarit, M., Fakhroueian, Z., Bahramian, A., & Sharareh, A. (2011). Inhibition of asphaltene precipitation by TiO2, SiO2, and ZrO2 nanofluids. *Energ. Fuel*., 25 (7), 3150-3156. DOI: 10.1021/ef2001635.

Mora, C., Franco, C. A., & Cortés, F. B. (2013). Uso de nanopartículas de sílice para la estabilización de finos en lechos empacados de arena Ottawa. *Rev. Inform. Técn*., 77 (1), 27. DOI: http://dx.doi.org/10.23850/22565035.42.

Montoya, T., Coral, D., Franco, C. A., Nassar, N. N., & Cortés, F. B. (2014). A novel solid–liquid equilibrium model for describing the adsorption of associating asphaltene molecules onto solid surfaces based on the "Chemical Theory". *Energ. Fuel*., 28 (8), 4963-4975. DOI: 10.1021/ef501020d.

Morrow, N. R. (1990). Wettability and its effect on oil recovery. *J. Petrol. Technol*. , 42 (12), 1476-1484. DOI: https://doi.org/10.2118/21621-PA.

Mullins, O. C. (2010). The Modified Yen Model. *Energ. Fuel*., 24 (4), 2179-2207. DOI: 10.1021/ef900975e.

Mullins, O. C. (2011). The asphaltenes. Ann. *Rev. Analyt. Chem*., 4, 393-418. DOI: 10.1146/annurev-anchem-061010-113849.

Mullins, O.C., Sheu, E.Y., Hammami, A. & Marshall, A.G. (2007). *Asphaltenes, heavy oils, and petroleomics*. Springer Science & Business Media.

Nassar, N. N. (2010). Asphaltene adsorption onto alumina nanoparticles: kinetics and thermodynamic Studies. *Energ. Fuel*., 24 (8), 4116-4122. DOI: 10.1021/ef100458g.

Nassar, N. N., Betancur, S., Acevedo, S.A., Franco, C., & Cortés, F.B., (2015a). Development of a population balance model to describe the influence of shear and nanoparticles on the aggregation and fragmentation of asphaltene aggregates. *Ind. Eng. Chem. Res.*, 54 (33), 8201-8211. DOI: DOI: 10.1021/acs.iecr.5b02075.

Nassar, N. N., Franco, C. A., Montoya, T., Cortés, F. B., & Hassan, A., (2015b). Effect of oxide support on Ni–Pd bimetallic nanocatalysts for steam gasification of nC 7 asphaltenes. *Fuel,* 156: 110-120. DOI: http://dx.doi.org/10.1016/j.fuel.2015.04.031.

Nassar, N. N., Hassan, A., Carbognani, L., Lopez-Linares, F., & Pereira-Almao, P., (2012). Iron oxide nanoparticles for rapid adsorption and enhanced catalytic oxidation of thermally cracked asphaltenes. *Fuel,* 95, 257-262. DOI: http://dx.doi.org/10.1016/j.fuel.2011.09.022.

Nassar, N. N., Hassan, A., & Pereira-Almao, P. (2011a). Application of nanotechnology for heavy oil upgrading: Catalytic steam gasification/cracking of asphaltenes. *Energ. Fuel*., 25 (4), 1566-1570. DOI: 10.1021/ef2001772.

Nassar, N. N., Hassan, A., & Pereira-Almao, P. (2011b). Metal oxide nanoparticles for asphaltene adsorption and oxidation. *Energ. Fuel*., 25 (3), 1017-1023. DOI: 10.1021/ef101230g.

Nassar, N. N., Montoya, T., Franco, C. A., Cortés, F. B., & Pereira-Almao, P.R. (2015c). A New model for describing the adsorption of asphaltenes on porous media at a high pressure and temperature under flow conditions. *Energ. Fuel*., 29 (7), 4210-4221. DOI: 10.1021/acs.energyfuels.5b00693.

Oliensis, G., (1935). The Oliensis spot test -- What justification is there for its use?, *Association of Asphalt Paving Technologists Proceedings.*

Pedersen, K. S., Christensen, P. L., & Shaikh, J. A. 2014. *Phase behavior of petroleum reservoir fluids*. (2 Edition). CRC Press.

Pernyeszi, T. & Dékány, I. (2001). Sorption and elution of asphaltenes from porous silica surfaces. *Colloid. Surf. A,* 194 (1-3), 25-39. DOI: http://dx.doi.org/10.1016/S0927-7757(01)00574-X.

Pernyeszi, T., Patzko, A., Berkesi, O., & Dékány, I. (1998). Asphaltene adsorption on clays and crude oil reservoir rocks. *Colloid. Surf. A*, 137 (1), 373-384. DOI. https://doi.org/10.1016/S0927-7757(98)00214-3.

Polanyi, M., (1914). Adsorption from the point of view of the Third Law of Thermodynamics. *Verh. Deut. Phys. Ges*, 16, 1012-1016.

Riffel, D. B., Schmidt, F., Belo, F. A., Leite, A. P. F., Cortés, F, Chejne, F, & Ziegler F. (2011). Adsorption of water on

grace silica gel 127B at low and high pressure. *Adsorption*, 17 (6), 977-984. DOI: doi:10.1007/s10450-011-9379-6.

Salathiel, R. (1973). Oil recovery by surface film drainage in mixed-wettability rocks. *J. Petrol. Technol*. , 25(10), 1,216-1,224.

Shang, J., Flury, M., Harsh, J. B., & Zollars, R. L. (2008). Comparison of different methods to measure contact angles of soil colloids. *J. Colloid Interf. Sci.,* 328 (2), 299-307. DOI: http://dx.doi.org/10.1016/j.jcis.2008.09.039.

Shayan, N.N. & Mirzayi, B. (2015). Adsorption and Removal of Asphaltene Using Synthesized Maghemite and Hematite Nanoparticles. *Energ. Fuel.,* 29(3), 1397-1406.

Sing, K. S. W. 1985. Reporting physisorption data for gas/solid systems with special reference to the determination of surface area and porosity (Recommendations 1984). *Pure App. Chem*., 57 (4), 603-619. DOI: https://doi.org/10.1351/pac198557040603.

Spiecker, P. M., Gawrys, K. L., & Kilpatrick, P.K. (2003a). Aggregation and solubility behavior of asphaltenes and their subfractions. *J. Colloid. Interf. Sci*., 267(1): 178-193.

Spiecker, P. M., Gawrys, K .L., Trail, C.B. & Kilpatrick, P. K. (2003b). Effects of petroleum resins on asphaltene aggregation and water-in-oil emulsion formation. *Colloid. Surf. A. Physicochem. Engine. Aspects,* 220 (1), 9-27. DOI: http://dx.doi.org/10.1016/S0927-7757(03)00079-7.

Szymula, M., & Marczewski, A. W. 2002. Adsorption of asphaltenes from toluene on typical soils of Lublin region. *Appl. Surf. Sci.,* 196 (1), 301-311. DOI: http://dx.doi.org/10.1016/S0169-4332(02)00068-5.

Van Oss, C. J. (2006). *Interfacial forces in aqueous media.* (2 Edition). Florida: CRC Taylor & Francis Group.

Wang, B . X., Zhao, Y., & Zhao, X. P. (2007). The wettability, size effect and electrorheological activity of modified titanium oxide nanoparticles. *Colloid Surface A Physicochem. Engin. Aspects*, 295 (1), 27-33. DOI: http://dx.doi.org/10.1016/j.colsurfa.2006.08.025.

Wu, J., Prausnitz, J. M., & Firoozabadi, A. (1998). Molecular-thermodynamic framework for asphaltene-oil equilibria. *AIChE J*., 44 (5), 1188-1199.

Zabala, R., Mora, E., Botero, O. F., Céspedes, C., Guarin, L., Franco, F. B., Cortes, F. B., Patiño, J. E., & Ospina, N. (2014). Nano-Technology for asphaltenes inhibition in Cupiagua South Wells, *IPTC 2014: Int. Petrol. Technol. Conf.*

## AUTHORS

**Farid Cortés**
Affiliation: *Facultad de Minas, Universidad Nacional de Colombia Sede Medellín*
e-mail: fbcortes@unal.edu.co

**Tatiana Montoya**
Affiliation: *Facultad de Minas, Universidad Nacional de Colombia Sede Medellín*
e-mail: ltmontoyac@unal.edu.co

**Sócrates Acevedo**
Affiliation: *Universidad Central de Venezuela, Caracas*
e-mail: socrates.acevedo@ciens.ucv.ve

**Nashaat Nassar**
Affiliation: *University of Calgary, Alberta, Canada.*
e-mail: nassar@ucalgary.ca

**Camilo Andrés Franco**
Affiliation: *Facultad de Minas, Universidad Nacional de Colombia Sede Medellín*
e-mail: caafrancoar@unal.edu.co